

51(200)
Se 46
v. 69
#2

BULLETIN OF THE
SEISMOLOGICAL SOCIETY
OF AMERICA

EDITORIAL COMMITTEE

THOMAS V. McEVILLY, Editor, Berkeley, California

HENRY J. DEGENKOLB, San Francisco

DAVID M. BOORE, Menlo Park, California

U.S. GEOLOGICAL SURVEY
MENLO PARK

AUG 13 1979

AUGUST 1979

	PAGE
Elementary Solutions to Lamb's Problem for a Point Source and Their Relevance to Three-Dimensional Studies of Spontaneous Crack Propagation	Paul G. Richards 947
Time Functions Appropriate for Nuclear Explosions	L. J. Burdick and D. V. Helmberger 957
Static Strike-Slip Faulting in a Horizontally Varying Crust	Kenneth D. Mahrer and Amos Nur 975
The Stabilization of Slip on a Narrow Weakening Fault Zone by Coupled Deformation-Pore Fluid Diffusion	J. W. Rudnicki 1011
Are Foreshocks Distinctive? Evidence from the 1966 Parkfield and the 1975 Oroville, California Sequences	W. H. Bakun and T. V. McEvilly 1027
Shear-Wave Velocity at the Base of the Mantle from Profiles of Diffracted SH Waves	Emile A. Okal and Robert J. Geller 1039
Frequency Dependence of Q_{scs}	Stuart A. Sipkin and Thomas H. Jordan 1055
The Effect of Appalachian Mountain Topography on Seismic Waves	Donald W. Griffiths and G. A. Bollinger 1081
Ground Motion on Alluvial Valleys Under Incident Plane SH Waves	Francisco J. Sánchez-Sesma and Jorge A. Esquivel 1107
Travel-Time and Amplitude Interpretation of Crustal Phases on the Refraction Profile DELTA-W, Utah	G. Müller and S. Mueller 1121
Shear Velocity Structure in the Eastern United States from the Inversion of Surface-Wave Group and Phase Velocities	Brian J. Mitchell and Robert B. Herrmann 1133
Interpretation of Short Period P-Wave Magnitude Anomalies at Selected LRSM Stations	Z. A. Der, T. W. McElfresh, and C. P. Mrazek 1149
The Horse Canyon Earthquake of August 2, 1975—Two-Stage Stress-Release Process in a Strike-Slip Earthquake	Stephen H. Hartzell and James N. Brune 1161
Tarbela Reservoir, Pakistan: A Region of Compressional Tectonics with Reduced Seismicity upon Initial Reservoir Filling	K. H. Jacob, W. D. Pennington, J. Armbruster, L. Seiber, and S. Farhatulla 1175
Estimate of the Focal Depth of Deep Earthquakes and Some Structural Implications for the Deep Seismic Activity in the Tyrrhenian Region	A. Bottari and B. Federico 1193
A Modified Form of the Gutenberg-Richter Magnitude-Frequency Relation	Jorge Lomnitz-Adler and Cinna Lomnitz 1209
An Interactive Epicenter Location Procedure for the RESMAC Seismic Array: II	Tomás Garza, Cinna Lomnitz, and Carlos Ruiz de Velasco 1215
A Bayesian Model for Seismic Hazard Mapping	C. P. Mortgat and H. C. Shah 1237
Determining Strong-Motion Duration of Earthquakes	Martin W. McCann, Jr. and Hareesh C. Shah 1253
Determination of Local Magnitude, M_L , from Seismoscope Records	Paul C. Jennings and Hiroo Kanamori 1267
<i>Letters to the Editor</i>	
Source Parameters of the Volvi-Langadhás Earthquake of June 20, 1978 Deduced from Body-Wave Spectra at Stations Uppsala and Kiruna	Ota Kulhánek and Klaus Meyer 1289
Active Seismic Focus Near Snyder, Texas	David B. Dumas 1295
Seismological Notes	1301
Fourth Award of the Medal of the Seismological Society of America	1305
Announcements	1309

062416

LOAN LIMIT

THE HORSE CANYON EARTHQUAKE OF AUGUST 2, 1975—TWO-STAGE STRESS-RELEASE PROCESS IN A STRIKE-SLIP EARTHQUAKE

BY STEPHEN HARTZELL AND JAMES N. BRUNE

ABSTRACT

A moderate strike-slip earthquake ($M_L = 4.8$) occurred on the San Jacinto fault system about 60 km northwest of the Salton Sea on August 2, 1975. Analysis of main shock and aftershock data suggest that stress release during this earthquake took place in two stages. During one stage faulting occurred over a relatively small source area (source radius of ~ 0.5 km), with a rapid dislocation rate (rise time ~ 0.1 sec), possibly associated with an asperity on the fault. During the second stage of faulting, the rupture front grew, but at a much slower rate (rise time ~ 10 sec), to a final source radius of ~ 1.0 km. The above model explains the larger moment estimate based on 20-sec surface waves compared to shorter period body-wave estimates, and also the apparent increase in source dimension with time. The model allows for large stress drops over small source dimensions, but when averaged over the final extent of the rupture plane, stress drops are much lower. The rupture of the asperity is characterized by a moment of 6.5×10^{22} dyne-cm and a stress drop of about 225 bars. The total moment is about 3.0×10^{23} dyne-cm with an averaged stress drop over the fault plane of approximately 90 bars and a dislocation of 25 cm. Observations similar to the ones reported on here have been noted for other earthquakes with a wide range of magnitudes, including: a few large earthquakes in Japan, the 1971 San Fernando earthquake and some of its aftershocks, the 1975 Oroville earthquake, and some swarm events in the Imperial Valley. These observations suggest that a two-stage rupture mechanism may be a fairly common occurrence in shallow faulting and may reflect possible large variations in stress over a length scale of kilometers within the crust.

INTRODUCTION

The Horse Canyon earthquake ($M_L = 4.8$) occurred on the San Jacinto fault system on August 2, 1975 approximately 60 km northwest of the Salton Sea. This earthquake is noteworthy because it was fairly well instrumented, and affords an opportunity to study the source mechanism of an earthquake in a relatively simple geological setting, predominantly hard, granitic rock. Such a location should reduce complications in the records due to scattering. Also, the Horse Canyon earthquake produced no obvious strain precursor at the Piñon Flat Geophysical Observatory (Berger and Wyatt, 1978), on the three-component laser strain meter just 13 km northeast of the epicenter. The mechanism of this earthquake is therefore important from an earthquake prediction standpoint.

The reported origin time is 0 hr 14 min 7.5 sec, with an epicenter of $33^\circ 31.4'N$, $116^\circ 33.5'W$ and a depth of 12 km (Pasadena). The epicenter lies near the trifurcation of the San Jacinto fault, southeast of Anza, California (see Figure 1). The fault-slip solution in Figure 1 is a lower hemisphere projection reported by Kanamori (1976). The shaded areas indicate compression. The strike and dip of the fault plane are 307.2° and 71.9° , respectively, and of the auxiliary plane, 42.2° and 75.0° , respectively. The solution is based on first motions from 28 Southern California stations and is fairly well constrained. Amplitudes from five stations in the Canadian network at distances greater than 20° , give an average body-wave magnitude of 4.3 (Hartzell, personal communication, 1976). Using 12-sec Rayleigh waves at eight

Canadian stations and the procedure of Marshall and Basham (1972), an average surface-wave magnitude of 3.6 is obtained. Using the m_b versus M_s plot of Marshall and Basham (1972), the Horse Canyon earthquake discriminates from explosions as expected. About a dozen aftershocks in the magnitude range from 1.0 to 2.0 were recorded at Palomar (PLM) 38 km from the epicenter, within the first 12 hr following the main shock.

The epicentral region is characterized by a high level of microearthquake activity

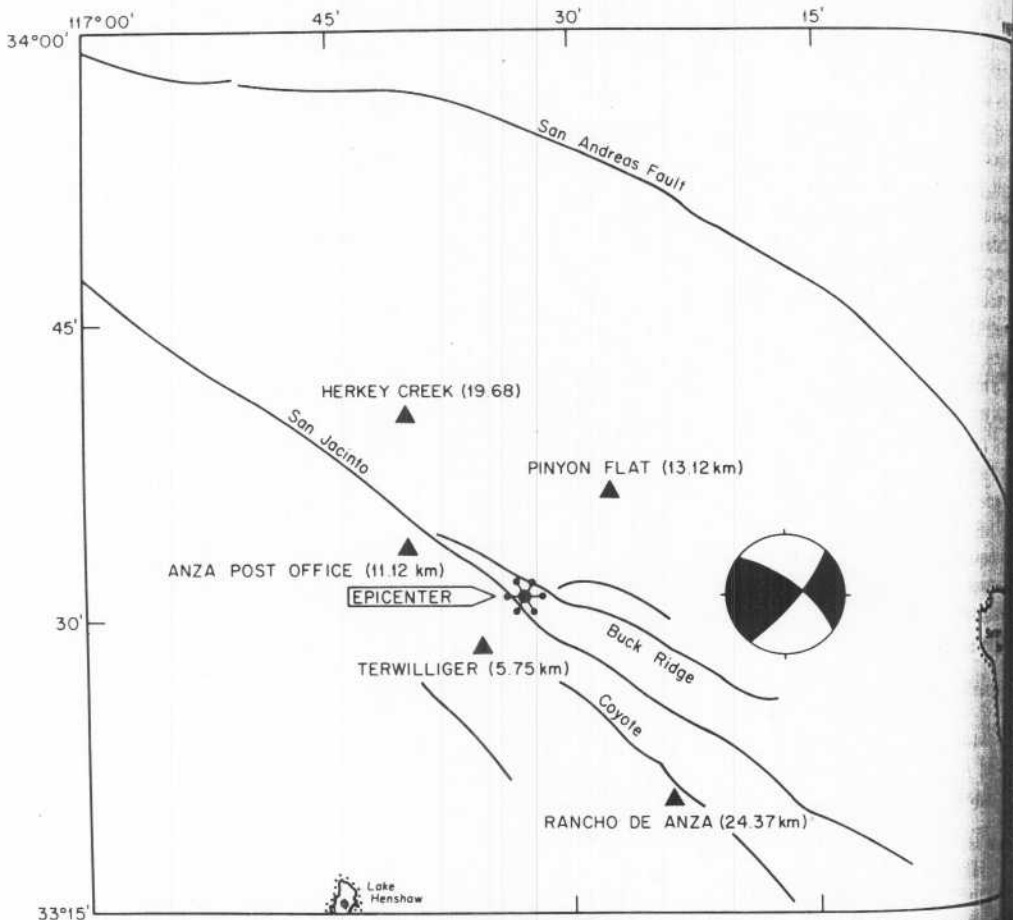


FIG. 1. Area map showing epicenter of Horse Canyon earthquake, strike-slip focal mechanism, and location of strong-motion instruments within 25 km of epicenter which triggered.

which occurs over a wide depth range from 3 to 15 km (Arabaz *et al.*, 1970). Hypocenters of the microearthquakes do not define any simple planar surfaces, rather are distributed over the width of the Coyote-San Jacinto-Buck Ridge fault zones (Arabasz *et al.*, 1970). Larger historic earthquakes along the 50-km length of the San Jacinto fault around the August 2, 1975 event, include one magnitude 4 earthquake, the March 25, 1937 "Terwilliger Valley" earthquake (Wood, 1937), and over a dozen magnitude 4 events.

EQUIPMENT AND DATA

Five strong motion accelerographs (standard SMA-1) were triggered by the main shock, within 25 km of the epicenter. None of the aftershocks triggered the strong motion instruments. The triangles in Figure 1 indicate the accelerograph locations.

Epicentral distances are given in parentheses. Records from these stations consist of 70-mm film with three components of acceleration: longitudinal (N45°W), transverse (S45°W), and vertical. The vertical accelerations are small in amplitude and are not important to this study. The two horizontal components from each of the five stations were digitized at a sample interval of 0.01 sec. and corrected for the response of the instrument (Trifunac and Lee, 1973). The results are shown in Figure 2. The Pinyon Flat, Anza Post Office, and Rancho de Anza stations triggered

CORRECTED ACCELERATION

LONGITUDINAL (N45W)

TRANSVERSE (S45W)

ANZA POST OFFICE

RANCHO DE ANZA

TERWILLIGER

PINYON FLAT

HERKEY CREEK

ONE SECOND

100 CM/SEC²

FIG. 2. Accelerograms for the strong-motion sites shown in Figure 1. All records have been corrected for the response of the instrument and start near the arrival of the S wave.

on the P wave, which means the first motion is lost (~0.1 sec), but the entire S wave is recorded. The Terwilliger and Herkey Creek stations triggered on the S wave, presumably near its onset. The largest acceleration of 130 cm/sec² occurred at the Anza Post Office station, 19 km from the hypocenter. The station with the next largest acceleration is Rancho de Anza, which is also the most distant of those in Figure 1. In addition, the period of maximum ground acceleration at Rancho de Anza is about a factor of two greater than the period of maximum acceleration at the other four stations. Both of the above observations are attributed to the amplification and high-frequency attenuation of the alluvium at the northwest end of the Borrego Valley, on which the Rancho de Anza station is situated.

In addition to the accelerograms for the main shock, aftershocks were recorded on a portable, digital system with a 5-sec natural period, horizontal seismometer.

The frequency response of the combined seismometer-recorder system is given in Figure 3 for several gain settings. The digital recorder has a sample rate of 128 samples/sec and is similar to the system described by Prothero (1976). The digital system was operated in a triggered mode with a delay line and usually recorded the first motion. Two sites were occupied; Pinyon Flat from 09:26Z to 14:48Z on August 2, and the upper end of Coyote Canyon for a period of 20 hr starting at 19:38Z on August 2. The seismometer was aligned in a NS orientation at the Pinyon Flat site and approximately perpendicular to the trend of the Coyote Fault (S45°W) at the Coyote Canyon site. The Pinyon Flat station is located about 150 m from the Pinyon

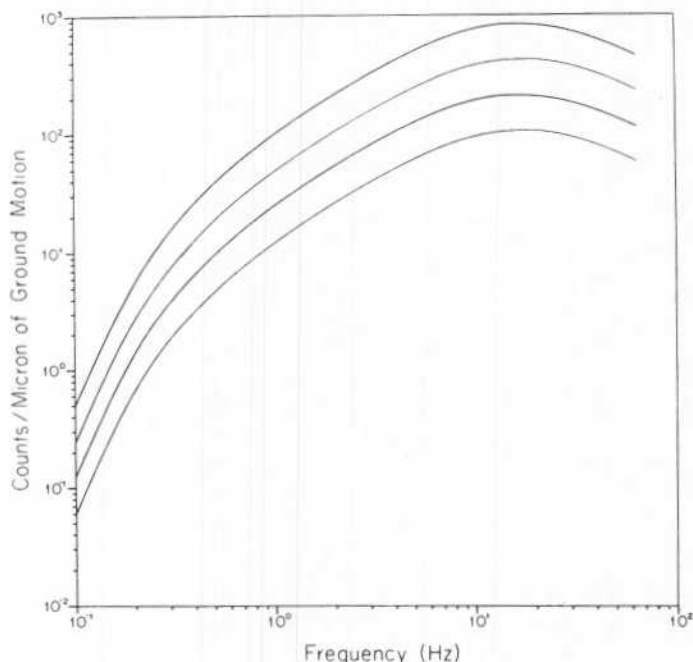


FIG. 3. Combined seismometer (period = 5 sec) and portable digital recorder response for five amplifier settings.

strong-motion accelerograph, which recorded the main shock. The Coyote Canyon station is 1.5 km NNW of the Terwilliger accelerograph.

Seven small aftershocks were recorded during the 5 hr of operation at the Pinyon Flat site. An additional nine aftershocks were recorded at the Coyote Canyon site. A few of the aftershock records (velocities) are shown in Figure 4. Also shown in comparison are the ground velocities for the main shock, obtained from the integrated acceleration records from the Pinyon Flat and Terwilliger stations (Figure 2). The main shock records have been rotated into the orientation of the aftershock data. The *S-P* times of 2.2 to 2.5 sec at Pinyon Flat are consistent with a source depth of about 12 km, given the above epicentral location. The downward motions at Pinyon are also consistent with the fault-plane solution of Figure 1.

SURFACE-WAVE ESTIMATE OF MOMENT

The Tucson, Arizona (TUC) WWSSN long-period vertical record for the Coyote Canyon earthquake has a clearly recorded Rayleigh wave (Figure 5). Surface-wave synthetics were generated using the method of Harkrider (1964, 1970). The fault-plane solution in Figure 1 and the average continental structure KHC2 (Table

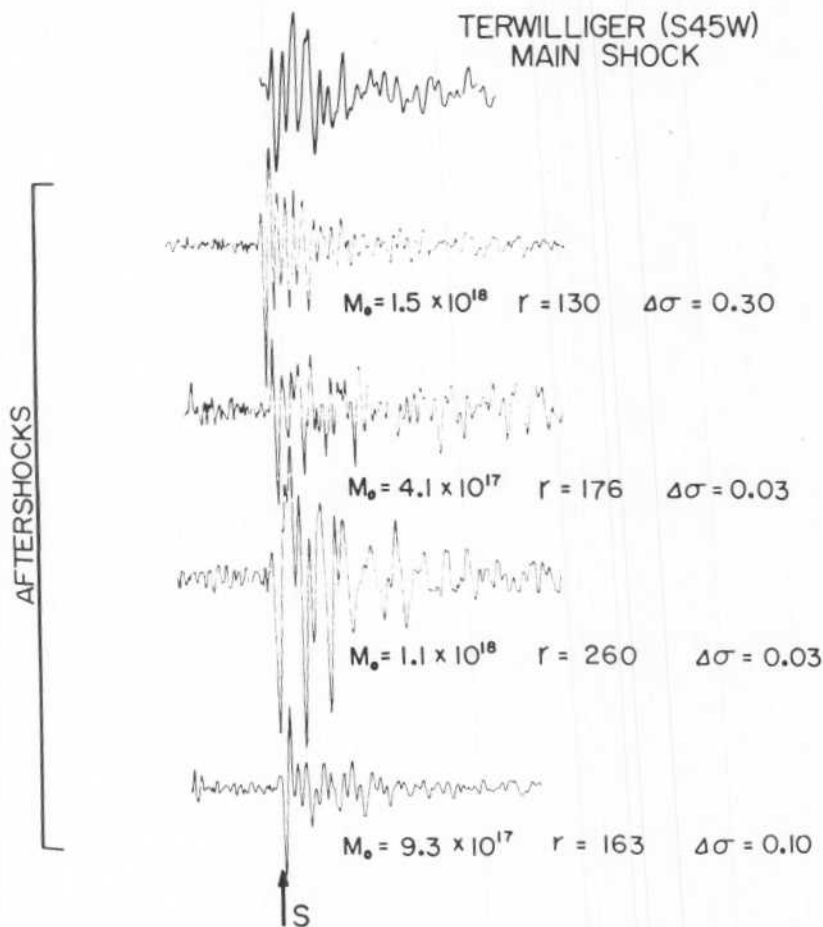
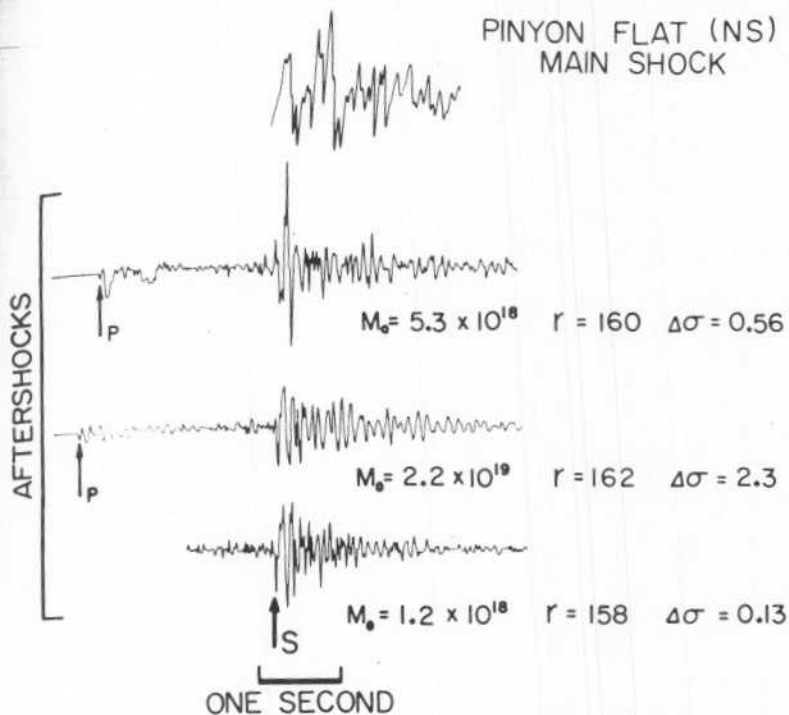


FIG. 4. Comparison of main-shock velocity records from the Pinyon Flat and Terwilliger strong-motion instruments with selected aftershock records (velocities) from the Pinyon Flat and Coyote Canyon portable digital recorder sites.

Hiroo Kanamori, personal communication) were used. Figure 5 shows a comparison between the observed record and synthetics for a point source with a step-source time function, a source depth of 12 km, and four different values of Q : 50, 100, 200 and 300. The leading, long-period part of the Tucson record is predominantly 20- to 30-sec energy, whose amplitude is less sensitive to the choice of Q than the shorter period energy. The long-period part of the synthetics yield moment estimates of 4.93, 4.05, 3.74, and 3.34×10^{23} dyne-cm, respectively, for the four values of Q . An alternative earth model was tried, model NTS-TUC from Bache *et al.* (1978). This

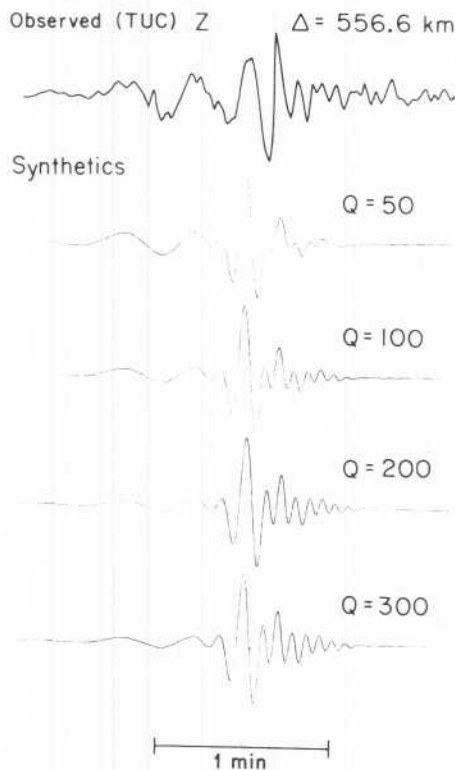


FIG. 5. TUC long-period vertical record and Rayleigh-wave synthetics for the earth structure in Table 1 and the fault-plane solution in Figure 1.

structure is based on the inversion of surface-wave data from Nevada Test Site explosions as recorded at Tucson. Model NTS-TUC gives moment estimates about 10 per cent less than model KHC2, with no better fit to the general wave form. Kanamori (1976) has also estimated the surface-wave moment of the Horse Canyon earthquake, using several different Q models for the TUC and BKS records. Kanamori's values yield an average moment of about 3.0×10^{23} dyne-cm, based on the longer period part of the records.

As a check on our calculations, the surface-wave synthetics obtained from Hartzell's program were compared with synthetics from the direct wave numerical integration program of Apsel and Luco (1978). Nearly identical results were obtained. The small differences are attributed to the different manner in which attenuation is handled in the two programs.

BODY-WAVE ESTIMATES OF SOURCE PARAMETERS

Using the shear waves from the strong-motion records, the spectral theory of Brune (1970, 1971) may be applied to obtain body-wave estimates of source parameters. We limit the analysis to the following three components: Anza Post Office, S45°W; Pinyon Flat, N45°W; and Terwilliger, N45°W. These components have been chosen because their orientation is such that the records should be primarily SH energy. Also, the epicentral distances are nearly the same as or less than the depth of the source, thus complications due to scattering and diffraction should be minimal. Figure 6 shows the associated displacement amplitude spectra (corrected for a Q of 250) and the chosen low- and high-frequency asymptotes. Table 2 summarizes the estimates of moment (M_0), source radius (r), and stress drop ($\Delta\sigma$), where the

TABLE 1
MODEL KHC2

Layer	Thickness (km)	α (km/sec)	β (km/sec)	ρ (gm/cm ³)
1	1.0	2.50	1.44	2.50
2	3.0	5.50	3.14	2.60
3	23.4	6.30	3.63	2.70
4	5.0	6.80	3.92	2.90
5	8.6	8.37	4.73	3.50
6	20.0	8.37	4.71	3.52
7	20.0	8.08	4.62	3.47
8	20.0	7.93	4.35	3.43
9	20.0	7.78	4.18	3.40
10	25.0	7.75	4.22	3.38
11	25.0	7.78	4.30	3.36
12	25.0	7.97	4.44	3.35
13	25.0	8.19	4.56	3.34
14	25.0	8.39	4.61	3.34
15	25.0	8.52	4.58	3.37
16	25.0	8.55	4.57	3.41
17	25.0	8.57	4.57	3.47
18	25.0	8.59	4.59	3.53
19	25.0	8.64	4.64	3.59

following expressions have been used (Thatcher and Hanks, 1973)

$$M = 4\pi\mu\beta\Omega_0 R/0.85; \quad r = 2.34\beta/2\pi f_c; \quad \Delta\sigma = (7/16) (M_0/r^3).$$

We have assumed a shear-wave velocity (β) of 3.5 km/sec and a rigidity (μ) of 3.0×10^{11} dyne/cm². The moment estimate from the Anza Post Office record is probably an overestimate, since this station is situated near the center of a small alluvial basin. The valley sediments will introduce an amplification not accounted for in the above calculation. Below we use a layered model in an attempt to obtain a better estimate. The Pinyon Flat and Terwilliger stations are located on granitic rock and should not have this problem. Because of an S-wave trigger, the Terwilliger record may underestimate the moment.

The displacement record, obtained by integrating the Anza Post Office accelerogram (Trifunac and Lee, 1973), was modeled with a point shear dislocation in a layered earth structure using the generalized ray method. The response of individual

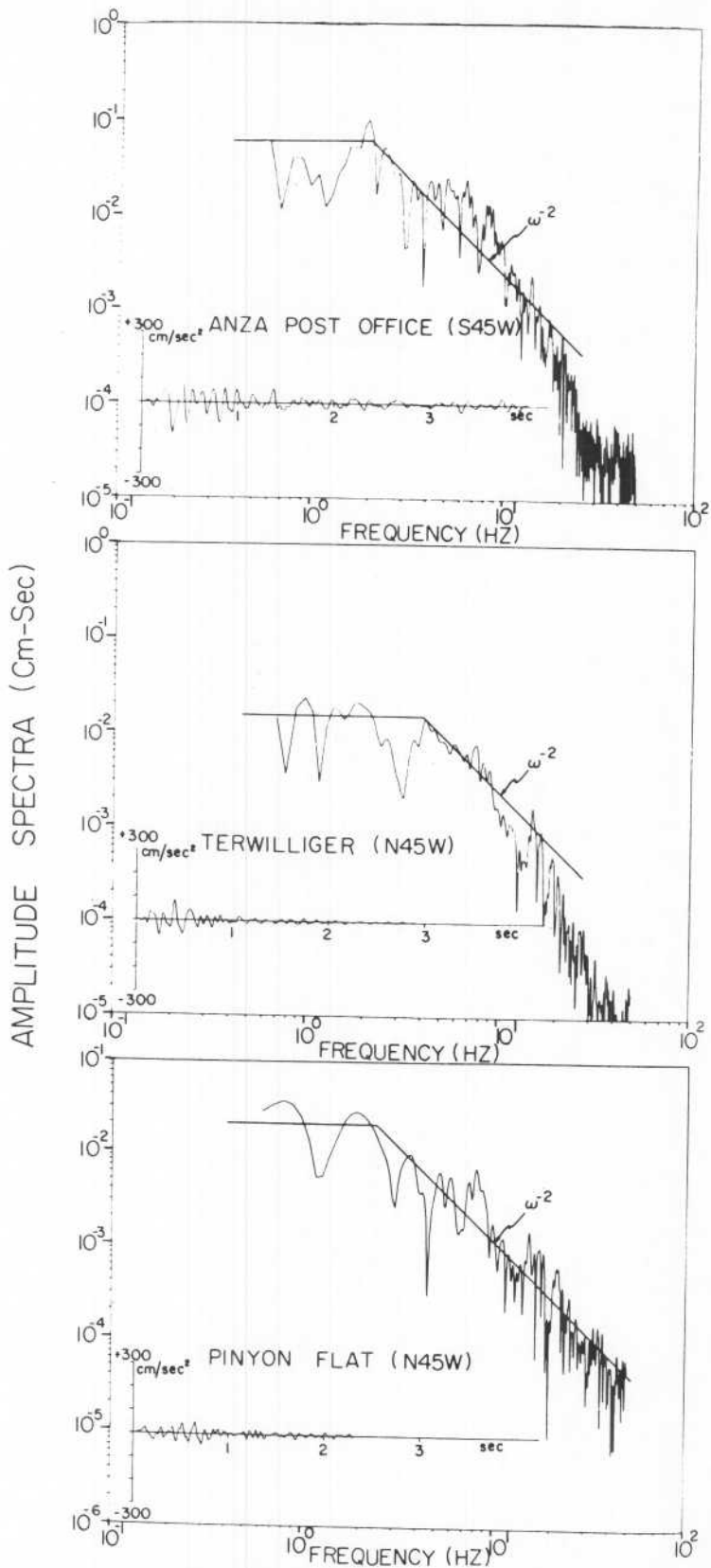


FIG. 6. Main-shock displacement amplitude spectra from the three close in strong-motion stations at Anza Post Office, Terwilliger, and Pinyon Flat.

generalized rays is calculated by the Cagniard-de Hoop technique, and summed (Helmberger, 1974). Figure 7 compares the Anza Post Office horizontal records with the generalized ray synthetics, for the earth structure in Table 3 and the fault-plane solution in Figure 1. The earth model used here is basically a sedimentary layer over a granitic half-space. The rise time on the fault is 0.15 sec. Synthetics for a single and a double event source are shown. Both the data and the synthetics have

TABLE 2
BODY-WAVE ESTIMATES OF SOURCE PARAMETERS

Component	Moment (dyne-cm)	Source Radius (m)	Stress Drop (bars)
Anza Post Office, S45°W	1.8×10^{23}	650	280
Pinyon Flat, N45°W	6.2×10^{22}	590	130
Terwilliger, N45°W	3.3×10^{22}	330	420

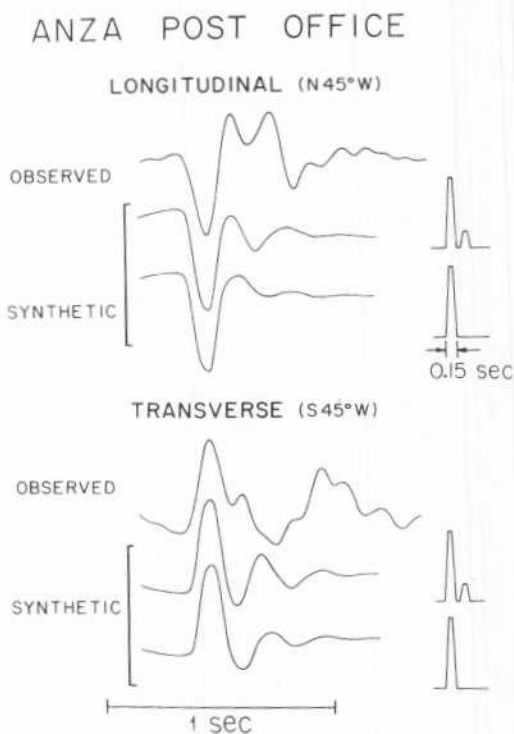


FIG. 7. Comparison of Anza Post Office main shock, horizontal displacements, and generalized ray synthetics for the structure in Table 3 and the fault-plane solution in Figure 1. The far-field source-time function is shown to the right of each synthetic.

been high-pass filtered with an Ormsby filter with roll-off frequency of 1.0 Hz and roll-off interval of 0.2 Hz. In addition, the synthetics have been attenuated assuming a Q of 250. Oscillations arriving later in the data, and not explained by the synthetics, are attributed to reflections from the edges of the valley (i.e., oscillations of the sedimentary basin). The moment inferred from the above modeling is 6.6×10^{22} dyne-cm. If we discount the Terwilliger estimate, because of an S -wave trigger, the preferred body-wave estimate of moment is 6.5×10^{22} dyne-cm. In comparison, the moment obtained by averaging spectral estimates from the horizontal components for all the stations in Figure 1 is 8.0×10^{22} dyne-cm.

COMPARISON OF AFTERSHOCKS WITH MAIN SHOCK

From the above analysis, there is about a factor of 4 to 6 discrepancy between moment estimated from 20-sec surface waves and body-wave estimate of moment at a period of less than a second. This difference seems too large to ascribe to error due to scattering, or uncertainties in the earth structure.

As stated above, the Pinyon Flat and Terwilliger accelerographs are located close to the sites occupied by the digital system used to record aftershocks. The comparison in Figure 4 between aftershock and main-shock records points out striking similarity. The duration and frequency content are similar, suggesting that the main shock was a simple event with a source dimension not a great deal larger than the small aftershocks. Spectral analysis of the aftershock records yields the indicated values of moment, source radius, and stress drop in Figure 4. The moment of the main shock is four to five orders of magnitude larger than the aftershock moments, yet the main-shock source radius, as inferred from body-wave analysis, is only ~ 3 times larger than the aftershock source radii.

The distribution of aftershocks should give a long-period estimate of the source dimension. Locations of aftershocks by Kanamori (1976) imply a source area of about 4.0 km^2 (over an approximately 2 by 2 km^2 area), significantly larger than the estimates in Table 2. The above data indicate larger estimates of source dimension at longer periods.

TABLE 3
ANZA POST OFFICE STRUCTURE

Thickness (km)	α (km/sec)	β (km/sec)	ρ (gm/cm ³)
0.1	2.50	1.44	2.50
0.4	5.50	3.14	2.60
—	6.30	3.63	2.70

DISCUSSION

In summary, the Horse Canyon earthquake is characterized by a local body-wave estimate of moment 4 to 6 times less than the surface-wave estimate of moment. The frequency content and duration of the strong-motion records for the main shock are very similar to that of the small aftershock records. Local body-wave analysis suggests that main shock and aftershock source dimensions are not greatly different. However, the distribution of aftershocks indicate a significantly larger source dimension.

Observations similar to the ones above have been reported for other earthquakes. Kanamori (1973) attributed larger moment estimates at longer periods, for some earthquakes in Japan, to afterslip or foreslip on the fault plane with a relatively slow dislocation velocity. Tucker and Brune (1977) found two spectral components at low frequencies, with an intermediate spectral slope of ω^{-1} , for about half of the $(M_L \approx 3.5 \text{ to } 4)$ San Fernando aftershocks. This spectral shape was attributed to either afterslip or foreslip, a growing rupture in time or space, or a partial stress drop model (Brune, 1970, 1971). Similar results were obtained for a swarm of earthquakes in the Imperial Valley (Hartzell and Brune, 1977) and the August 1975 Oroville earthquake (Hart *et al.*, 1977).

In the case of the Horse Canyon earthquake, the data suggest a particular rupture release process diagrammatically shown in Figure 8. Faulting initiates with a rupture over a relatively small area (source radius $\sim 0.5 \text{ km}$) with a rapid dislocation (rise time $\sim 0.1 \text{ sec}$). This first phase of the rupture accounts for the simple

the main shock records and the smaller body-wave estimate of source radius and moment. If the rupture from them continues to expand, but at a much slower dislocation rate (rise time ~ 10 sec), most of the energy radiated will be at surface-wave periods. This phase of the rupture accounts for the larger surface-wave estimate of the moment and the larger source dimension based on the distribution of aftershocks.

In the above rupture model we have reasoned that there was an initial sharp break, followed by slip over a larger area. Actually we have not determined at what stage of the rupture process the sharp break occurred. Sliding might have first taken place over much of the 4 km^2 fault surface, followed by the breaking of an asperity. However, the Pinyon Flat strain meter record suggests that faulting initiated with

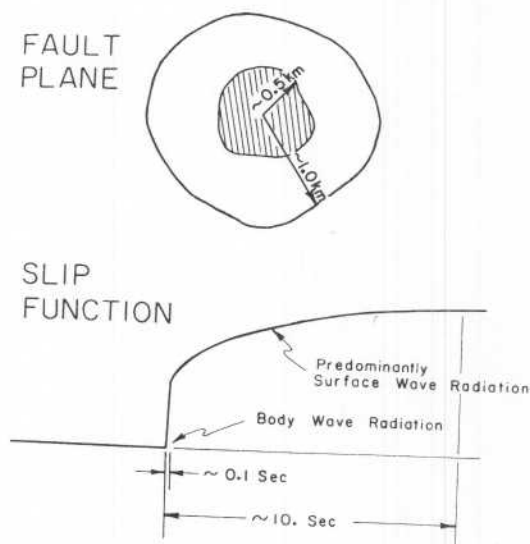


Fig. 8. Diagrammatic illustration of a possible mechanism for the Horse Canyon earthquake.

the breaking of the asperity. With a sample interval of 2 sec and an instrumental noise level of 75 counts (one fringe), all three strain components (NS, NW, and EW) show variations of less than 19 counts ($1/4$ fringe) for at least 60 sec prior to the arrival of the initial earthquake phase. Only the NS component remained on scale during the earthquake. The first sample on the NS component different from the pre-earthquake level shows a jump of 12 counts. The next sample, 2 sec later, is 917 counts above the pre-earthquake level. For an average P -wave velocity of 6.1 km/sec and the above quoted values for the hypocenter and the origin time, the calculated arrival time of the direct P -wave from the source is 1.5 sec before the 12-count sample. The absolute time of the strain data is good to ± 0.5 sec. The origin time given above is based largely on the trigger and S times at the strong-motion asperity. Therefore, the arrival time of the first signal on the strain record is consistent with the arrival time of the direct P wave from the breaking of the asperity. If the long-period motion on the fault had taken place first, one would expect to see a clear signal about 10 sec earlier in the strain record. Thus we conclude that this earthquake was not preceded by a long-period precursor like that suggested for some deep earthquakes (Gilbert and Dziewonski, 1975.)

In the above model large stress drops, several hundred bars or even kilobars, occur over relatively small source dimensions (≤ 1 km), while the stress averaged over the final extent of the fault plane will be much less. This may be the case for the high stress drop event of 636 bars ($M_L = 4.3$) reported by Hartzell and Brune (1977) from the January 1975 Brawley earthquake swarm. Evidence of a similar faulting mechanism for the 1971 San Fernando earthquake is given by Hanks (1974), in which rupture begins with massive but localized failure accompanied by a high stress drop. For the Horse Canyon earthquake, a moment of 6.5×10^{22} dyne-cm and source radius of 0.5 km gives a stress drop of 225 bars for the rupture of the asperity. Continued expansion of the rupture plane increases the moment and source radius to 3.0×10^{23} dyne-cm and 1.13 km ($=4$ km² source area), respectively, and decreases the average stress drop over the fault plane to about 90 bars. The final average dislocation is about 25 cm.

The lack of a strain precursor at the Piñon Flat Observatory prior to the Horse Canyon earthquake may be due to the small area of the asperity. Strain could be continually relieved in the area by creep and microearthquakes, except for a few isolated asperities, which "hang up" and form points of stress concentration. As an asperity will eventually break through, with a high stress drop over a small source dimension. The rupture may continue to expand outward, but subsequently will stop out in the surrounding region of lower effective stress. Major earthquakes, such as the 1940 Imperial Valley earthquake (Trifunac and Brune, 1970), often appear as multiple events, which could be a cascading rupture of several such asperities.

ACKNOWLEDGMENTS

Jerry King and William Prothero assisted in the field work. The strong-motion records were supplied by the Engineering Department of the California Institute of Technology. Hiroo Kanamori kindly supplied results prior to publication. This work was supported in part by National Science Foundation Grant DES74-03188 and National Aeronautics and Space Administration Grant NGR 05-009-246, and a contribution of Scripps Institution of Oceanography.

REFERENCES

- Aspel, R. J. and J. E. Luco (1978). Dynamic Green functions for a layered half-space. *UCSD Report*, Department of Applied Mechanics and Engineering Science, University of California at San Diego.
- Arabas, W. J., James N. Brune, and Gladys R. Engen (1970). Locations of small earthquakes near the trifurcation of the San Jacinto fault southeast of Anza, California. *Bull. Seism. Soc. Am.* **60**, 617-624.
- Bache, T. C., W. L. Rodi, and D. G. Harkrider (1978). Crustal structure inferred from Rayleigh wave signatures of NTS explosions. *Bull. Seism. Soc. Am.* **68**, 1399-1413.
- Berger, J. and F. Wyatt (1978). Some remarks on the base length of tilt and strain measurements. *Proceedings from Conference on Measurement of Ground Strain Phenomena Related to Earthquake Prediction*, Sept. 7-9, U.S. Geol. Survey Publ.
- Brune, J. N. (1970). Tectonic stress and the spectra of seismic shear waves from earthquakes. *J. Geophys. Res.* **75**, 4997-5007.
- Brune, J. N. (1971). (Correction) Tectonic stress and the spectra of seismic shear waves from earthquakes. *J. Geophys. Res.* **76**, 5002.
- Gilbert, F. and A. M. Dziewonski (1975). An application of normal mode theory to the retrieval of structural parameters and source mechanisms from seismic spectra. *Phil. Trans. Roy. Soc. London Ser. A*, **278**, 187-269.
- Hanks, T. C. (1974). The faulting mechanism of the San Fernando earthquake. *J. Geophys. Res.* **79**, 1215-1229.
- Harkrider, D. G. (1964). Surface waves in multilayered elastic media. Part I. Rayleigh and Love waves from buried sources in a multilayered elastic halfspace. *Bull. Seis. Soc. Am.* **54**, 627-679.
- Harkrider, D. G. (1970). Surface waves in multilayered elastic media. Part II. Higher mode spectra and spectral ratios from point sources in plane layered earth models. *Bull. Seism. Soc. Am.* **60**, 1987.

- Hart, R. S., R. Butler, and H. Kanamori (1977). Surface-wave constraints on the August 1, 1975, Oroville earthquake. *Bull. Seism. Soc. Am.* **67**, 1-7.
- Hartwell, S. H. and James N. Brune (1977). Source parameters for the January, 1975 Brawley-Imperial Valley earthquake swarm. *Pageoph* **115**, 333-355.
- Helmberger, D. V. (1974). Generalized ray theory for shear dislocations, *Bull. Seism. Soc. Am.* **64**, 45-64.
- Kanamori, H. (1973). Mode of strain release associated with major earthquakes in Japan, *Ann. Rev. Earth Planet Sci.* **1**, 213-239.
- Kanamori, H. (1976). California Institute of Technology Final Technical Report, October 1, 1975 to September 30, 1976. U.S. Geol. Surv. Contract 14-08-0001-15254.
- Marshall, P. D. and P. W. Basham (1972). Discrimination between earthquakes and underground explosions employing an improved M_s scale, *Geophys. J.* **28**, 431-458.
- Prothero, W. A. (1976). A portable digital seismic recorder with event recording capacity, *Bull. Seism. Soc. Am.* **66**, 979-985.
- Thatcher, W. and T. C. Hanks (1973). Source parameters of southern California earthquakes, *J. Geophys. Res.* **78**, 8547-8576.
- Trifunac, M. D. and J. N. Brune (1970). Complexity of energy release during the Imperial Valley, California, earthquake of 1940, *Bull. Seism. Soc. Am.* **60**, 137-160.
- Trifunac, M. D. and V. Lee (1973). Routine computer processing of strong-motion accelerograms, Earthquake Eng. Res. Lab., Calif. Inst. of Tech., Pasadena.
- Tucker, B. E. and J. N. Brune (1977). Source mechanism and m_s - M analysis of aftershocks of the San Fernando earthquake, *Geophys. J.* **49**, 371-426.
- Wood, H. O. (1937). The Terwilliger Valley earthquake of March 25, 1937, *Bull. Seism. Soc. Am.* **27**, 305-312.

SEISMOLOGICAL LABORATORY
CALIFORNIA INSTITUTE OF TECHNOLOGY
PASADENA, CALIFORNIA 91125 (S.H.H.)

UNIVERSITY OF CALIFORNIA, SAN DIEGO
INSTITUTE OF GEOPHYSICS AND PLANETARY PHYSICS
SCRIPPS INSTITUTION OF OCEANOGRAPHY
LA JOLLA, CALIFORNIA 92093 (J.N.B.)

MANUSCRIPT RECEIVED SEPTEMBER 28, 1978